THE JOURNAL OF BIOLOGICAL CHEMISTRY
Vol. 280, No. 26, Issue of July 1, pp. 24978–24986, 2005

Printed in U.S.A.

Sites of Tau Important for Aggregation Populate β-Structure and Bind to Microtubules and Polyanions*[S]

Received for publication, February 10, 2005, and in revised form, April 8, 2005
Published, JBC Papers in Press, April 26, 2005, DOI 10.1074/jbc.M501565200

Marco D. Mukrasch‡§, Jacek Biernat¶, Martin von Bergen¶, Christian Griesinger‡, Eckhard Mandelkow¶, and Markus Zweckstetter‡‖

From the ‡Department for NMR-based Structural Biology, Max Planck Institute for Biophysical Chemistry, Am Fassberg 11, 37077 Göttingen, Germany and the ¶Max Planck Unit for Structural Molecular Biology c/o DESY, Notkestrasse 85, 22607 Hamburg, Germany

The aggregation of the microtubule-associated tau protein and formation of "neurofibrillary tangles" is one of the hallmarks of Alzheimer disease. The mechanisms underlying the structural transition of innocuous, natively unfolded tau to neurotoxic forms and the detailed mechanisms of binding to microtubules are largely unknown. Here we report the high-resolution characterization of the repeat domain of soluble tau using multidimensional NMR spectroscopy. NMR secondary chemical shifts detect residual β-structure for 8–10 residues at the beginning of repeats R2–R4. These regions correspond to sequence motifs known to form the core of the cross-β-structure of tau-paired helical filaments. Chemical shift perturbation studies show that polyanions, which promote paired helical filament aggregation, as well as microtubules interact with tau through positive charges near the ends of the repeats and through the β-forming motifs at the beginning of repeats 2 and 3. The high degree of similarity between the binding of polyanions and microtubules supports the hypothesis that stable microtubules prevent paired helical filament formation by blocking the tau-polyanion interaction sites, which are crucial for paired helical filament formation.

Alzheimer disease is characterized by abnormal protein deposits in the brain, such as amyloid plaques or neurofibrillary tangles, formed by fibrous assemblies of the Aβ peptide (1) or of the microtubule (MT)[1]-associated tau protein (2). These aggregates are thought to be toxic to neurons, either by causing some toxic signaling defect or by obstructing the cell interior. Therefore, one of the top priorities in Alzheimer research is to understand the reasons for the pathological aggregation and to find methods to prevent it. Although the structural principles governing Aβ aggregation are known in some detail, little is known for the tau protein.

Tau is a microtubule-associated protein that regulates MT stability, neurite outgrowth, and other MT-dependent functions. The three or four repeats in the C-terminal half of the protein and the flanking proline-rich basic domains are known to be involved in MT binding (3). The affinity is regulated by phosphorylation particularly at K*X*GS-motifs in the repeats (4). Interestingly the same phosphorylation sites have an inhibitory influence on aggregation (5). Unbound tau can assemble into Alzheimer-like paired helical filaments (PHFs) whose polymerization can be enhanced by oxidation of SH groups and by polyanions (*e.g.* heparin, poly-Glu (6)). On the other hand, tau has a hydrophilic character, is highly soluble, and belongs to the class of natively unfolded proteins with no apparent ordered secondary structure detectable by far-UV CD or Fourier-transform infrared spectroscopy (7, 8). Therefore, it is unclear why tau should aggregate in a specific manner and what structural principles could be responsible for this.

Tau can aggregate as an intact protein, 352–441 residues in length (depending on isoform), so that all six tau isoforms are found in Alzheimer PHFs (9). The isoforms differ by two inserts near the N-terminal end and the presence of either four or three imperfect repeat sequences in the C-terminal half of the protein (see Fig. 1). The region comprising the repeat sequences forms the core of PHFs (10) and also promotes PHF assembly *in vitro* (11, 12). For PHF aggregation two hexapeptides at the beginning of the second and third repeats (^{275}VQIINK^{280} and ^{306}VQIVYK^{311}) are crucial. These are able to initiate the aggregation of tau into *bona fide* paired helical filaments with cross-β-structure and thereby represent minimal tau-tau interaction motifs (13, 14).

Because tau is a highly flexible protein, it has resisted all attempts at crystallization for a high-resolution x-ray structure. X-ray analyses exist only in the form of solution scattering (confirming the unfolded nature of the protein, (7)) and fiber diffraction (confirming the cross-β-structure of PHFs, (13)). We have now applied NMR spectroscopy as an alternative approach to structural studies. Here we report the high-resolution characterization of the repeat domain of tau, in which either all four repeats are present (K18) or repeat two has been deleted (K19), corresponding to the adult and fetal tau isoforms htau40 and htau23 (see Fig. 1). Our findings show that the repeat domain of soluble tau contains regions of residual β-structure that have the potential to serve as seeds for aggregation of tau into PHFs, and we identify residues involved in the interaction with MTs and with polyanions that promote PHF-aggregation.

EXPERIMENTAL PROCEDURES

Expression of Recombinant Tau Constructs and Isotope Labeling—Human tau constructs were expressed in the vector pNG2 (a derivative

* This work was supported by the Max Planck Society (to E. M. and C. G.), the European Union through Understanding Protein Misfolding and Aggregation by NMR (to M. Z.), the Fonds der Chemischen Industrie, and the Deutsche Forschungsgemeinschaft (DFG), through GK 782 (to C. G.), and through a DFG Emmy Noether Fellowship (to M. Z.) (ZW 71/1-4). The costs of publication of this article were defrayed in part by the payment of page charges. This article must therefore be hereby marked "*advertisement*" in accordance with 18 U.S.C. Section 1734 solely to indicate this fact.

[S] The on-line version of this article (available at http://www.jbc.org) contains supplemental Figs. S1, S2, and S3 and supplemental Table S1.

§ Recipient of a Boehringer Ingelheim fellowship.

‖ To whom correspondence should be addressed. Tel.: 49-551-201-2220; Fax: 49-551-201-2202; E-mail: mzwecks@gwdg.de.

[1] The abbreviations used are: MT, microtubule; PHF, paired helical filament; MES, 4-morpholineethanesulfonic acid; Pipes, 1,4-piperazinediethanesulfonic acid; HSQC, heteronuclear single quantum correlation.

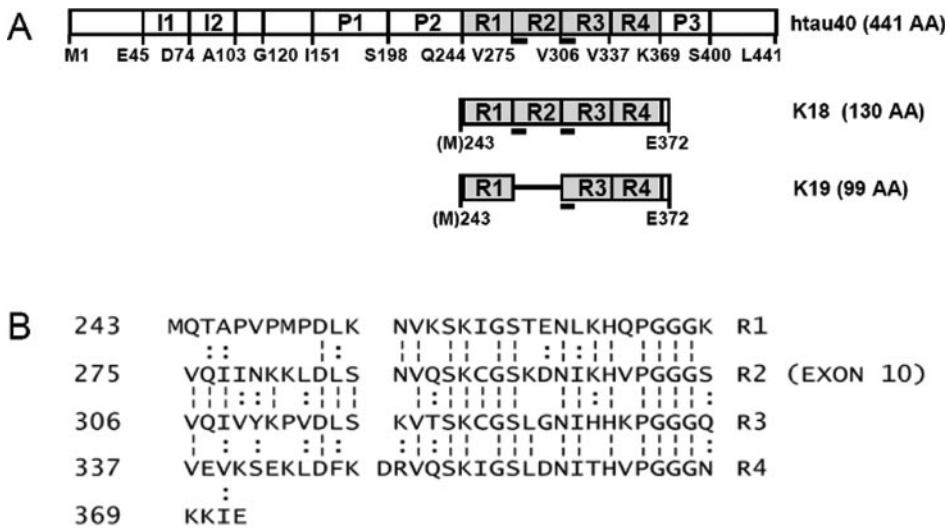

FIG. 1. *A*, tau isoforms and tau-derived constructs. The bars show the tau isoform htau40 and the constructs K18 and K19. The isoform htau40 is the largest one in the human central nervous system (441 residues). According to the isoform the C-terminal half contains three or four pseudorepeats (~31 residues each, R1–R4, *gray shade*), which are involved in MT binding and form the core of PHFs. The constructs K18 and K19 represent the repeat domains of htau40, comprising four repeats or three repeats, respectively. The positions of the hexapeptides ^{275}VQIINK^{280} and ^{306}VQIVYK^{311} in R2 and R3 are *underlined*. Domain boundaries are labeled by the residue numbers. *B*, amino acid sequence of the repeat domain of tau. The sequence shows the four-repeat construct K18, repeat R2 (275–305) is absent in K19, corresponding to the alternative splicing of exon 10. The overall character of the protein is hydrophilic and basic. Each repeat terminates with a characteristic PGGG motif. Identical amino acids in all repeats are marked by a *dashed line*; similar amino acids are indicated by a *double dot*.

of pET-3a, Merck-Novagen, Darmstadt) in *Escherichia coli* strain BL21(DE3) as described (Gustke *et al.* (3)) (see Fig. 1). K18 comprises all four repeats of the largest tau isoform (residues Gln^{244}-Glu^{372} plus initial Met^{243}), K19 is similar but lacks the second repeat, corresponding to fetal tau (residues Met^{243} + Gln^{244}-Lys^{274}, Val^{337}-Glu^{372}, without R2 = Val^{275}-Ser^{305}). The expressed proteins were purified from bacterial extracts by making use of the heat stability of the protein and by FPLC SP-Sepharose chromatography (Amersham Biosciences). To label the tau proteins with ^{15}N and ^{13}C stable isotopes, the *E. coli* culture expressing K18 protein was grown in a M9 minimal medium with $^{15}NH_4Cl$ (1 g liter^{-1}) and ^{13}C glucose (4 g liter^{-1}) (Campro Scientific), and the *E. coli* culture expressing K19 protein was grown on rich growth medium based on chemolithoautotrophic bacteria labeled with ^{13}C and ^{15}N isotopes (Silantes). Protein samples uniformly enriched in ^{15}N were prepared by growing *E. coli* bacteria in minimal medium containing 1 g liter^{-1} of $^{15}NH_4Cl$.

The cell pellets were resuspended in boiling extraction buffer (50 mM MES, 500 mM NaCl, 1 mM $MgCl_2$, 1 mM EGTA, 5 mM dithiothreitol, pH 6.8) complemented with a protease inhibitor mixture. The cells were disrupted with a French pressure cell and subsequently boiled for 20 min. The soluble extract was isolated by centrifugation, the supernatant was dialyzed against two changes of cation exchange chromatography buffer A (20 mM MES, 50 mM NaCl, 1 mM EGTA, 1 mM $MgCl_2$, 2 mM dithiothreitol, 0.1 mM phenylmethylsulfonyl fluoride, pH 6.8) and loaded on an FPLC SP-Sepharose column. The proteins were eluted by a linear gradient of cation exchange chromatography buffer B (20 mM MES, 1 M NaCl, 1 mM EGTA, 1 mM $MgCl_2$, 2 mM dithiothreitol, 0.1 mM phenylmethylsulfonyl fluoride, pH 6.8). NMR samples contained 0.9–1.5 mM ^{15}N- or ^{15}N/^{13}C-labeled protein in 95% H_2O, 5% D_2O, 50 mM phosphate buffer, pH 6.8, with 1 mM dithiothreitol.

Preparation of MTs—Porcine brain tubulin was purified as described (15) and incubated at concentrations higher than 200 μM in MT assembly buffer (100 mM Pipes, pH 6.9, 1 mM EDTA, 1 mM $MgSO_4$, 1 mM dithiothreitol) in the presence of 1 mM GTP at 37 °C for 5 min. After addition of 100 μM Paclitaxel (Sigma-Aldrich) the polymerization was performed for 20 min at 37 °C.

Electron Microscopy—Proteins were diluted to a concentration of ~0.1 mg/ml, placed on 600-mesh carbon-coated copper grids for 1 min, washed with two drops of H_2O, and negatively stained with 2% uranyl acetate for 45 s. The specimen were examined in a Philipps 12M electron microscope at 100 kV.

NMR Spectroscopy—NMR spectra were acquired at 5 °C on Bruker DRX 800, Avance 600, and DRX 600 NMR spectrometers. Aggregation did not occur under these low temperature conditions. NMR data were processed and analyzed using nmrPipe (16) and Sparky 3. Three-dimensional triple-resonance experiments were collected to obtain sequence-specific assignments for the backbone of K18 and K19 (supplemental Table S1). Secondary shift values were calculated as the differences between the measured C^α/C' chemical shifts and the empirical random coil value for the appropriate amino acid type at pH 3.0 (17). Random coil values for histidines, glutamates, and aspartates were taken from Wishart *et al.* (18), as the chemical shifts of these residues are particularly sensitive to pH, and the pH in the studies by Wishart *et al.* (18) (pH 5.0) is more similar to the one used here (pH 6.9). To estimate the β-sheet propensity in contiguous segments of tau, the observed C^α secondary shifts were normalized by the empirically determined secondary shift expected for that residue type in a fully β-sheet conformation (18), summed, and normalized by the number of residues in the segment.

Tau-polyanion titrations were carried out with uniformly ^{15}N-labeled protein containing 0.2 mM (heparin titration) and 0.3 mM (poly-Glu titration) K18, and 0.12 mM (heparin titration) and 0.14 mM (poly-Glu titration) K19 at pH 6.8. Heparin (average molecular weight 3000, ~5.8 disaccharide subunits, charge/subunit ~2.5, ~0.31 z/Å) and poly-Glu (average molecular weight 10,000, 7–8 Glu residues, 7–8 negative net charge, in extended conformation 0.33 z/Å) were from Sigma. Complex formation was monitored by recording two-dimensional ^{1}H-^{15}N HSQC spectra for increasing polyanion concentrations (in mM): 0.03, 0.06, 0.15, 0.3, 0.58, 1.37, and 2.53 (K18 with heparin), 0.008, 0.015, 0.03, 0.072, 0.142, 0.28, 0.68, 1.3, 2.4, and 4.3 (K18 with poly-Glu), 0.008, 0.015, 0.03, 0.07, 0.14, 0.28, 0.67, and 1.3 (K19 with heparin), and 0.015, 0.03, 0.074, 0.146, 0.29, 0.70, 1.35, and 2.49 (K19 with poly-Glu). For tau-MT titrations NMR samples contained 0.13 and 0.14 mM uniformly ^{15}N-labeled K18 and K19, respectively. Complex formation was monitored at 5 and 20 °C for MT concentrations ($\alpha\beta$-tubulin dimers) of 26.5, 79.5, and 159.0 μM in the K18 titrations, and 2.8, 5.4, 20.0, 35.0, and 84.3 μM in the K19 titration. Normalized weighted average chemical shift differences for amide ^{1}H and ^{15}N chemical shifts upon polyanion/MT binding were calculated using $\Delta_{av}(NH) = [(\Delta H^2 + (\Delta N/5)^2)/2]^{1/2}$, where ΔH and ΔN are the differences between the free and bound chemical shifts.

RESULTS

Backbone Resonance Assignment of K18 and K19—NMR resonances in ^{1}H-^{15}N HSQC spectra of the tau repeat domain constructs K18 and K19, uniformly labeled with ^{15}N, were recorded at 5 °C and pH 6.9. The resonances were sharp and showed only a limited dispersion of chemical shifts, reflecting a high degree of backbone mobility and unfolded nature, in agreement with CD and FTIR measurements (7, 13). To enable a study of the structure and dynamics of tau with atomic resolution, the assignment of the NMR resonances was required. Assignment of globular proteins with a molecular mass

below 15 kDa is straightforward today using multidimensional NMR techniques. Backbone assignment of K18 (130 residues) and K19 (99 residues) was complicated, however, by the limited dispersion of NMR resonances because of the absence of well defined secondary and tertiary structure elements. In addition, only five amino acid types make up more than 50% of the primary sequence, and these amino acids are arranged in sequence motifs that occur repetitively, further increasing NMR signal overlap. Therefore, an unambiguous assignment was not possible just relying on the conventional three-dimensional spectra HNCO, HN(CA)CO, HNCACB and CBCA(CO)NH (19). A high-resolution (HA)CANNH (20) together with three-dimensional HNN and HN(C)N experiments were required (21). With these NMR spectra the backbone resonance assignment of K18 and K19 could be achieved in an iterative fashion based on automatic assignment using the program MARS (22) and manual assignment mainly relying on the HNN experiment. The sequence motif PGGG, which is located characteristically at the C-terminal end of each of the four repeats, caused the biggest problems. Because of severe chemical shift overlap, it was only possible to assign Gly^{273}, Gly^{304}, and Gly^{335}. The resonances of the remaining glycines within these motifs could be identified in the spectra but not unambiguously assigned to one of the repeats. Otherwise, all ^{1}H, ^{15}N, $^{13}C^{\alpha}$, $^{13}C^{\beta}$, and $^{13}C'$ chemical shifts were assigned in both K18 and K19.

Soluble Tau Contains Residual β-Structure—NMR chemical shifts, in particular of C^{α} and C' atoms, are very sensitive probes of secondary structure both in globular and unfolded proteins (Ref. 23 and Wishart *et al*. (18)). These shifts show small but distinct deviations from random coil values for both K18 and K19 (Fig. 2). In the case of K18, continuous stretches (containing more than six amino acids) of negative C^{α} secondary chemical shifts were found for residues Lys^{274}-Leu^{284}, Ser^{305}-Leu^{315}, and Gln^{336}-Asp^{345} (numbering according to the longest isoform htau40), indicative of nascent β-structure (Fig. 2*A*). These stretches lie at the beginning of repeats R2, R3, and R4, downstream from PGGG motifs and encompass the hexapeptide motifs VQIINK and VQIVYK known to be important for the abnormal aggregation of tau into PHFs (8). In case of C', negative secondary chemical shifts were detected for a similar range of residues, Gly^{273}-Leu^{282}, Gly^{304}-Asp^{314}, and Gly^{335}-Asp^{345} (supplemental Fig. S1). It is notable that the preponderance of negative secondary chemical shifts persists even at the beginning of the less homologous repeats R1 (residues Ala^{246}-Leu^{253}) and R5 (Asn^{368}-Ile^{371}). In the case of R1 this is likely not because of a propensity to form β-structure but rather because of the occurrence of three prolines (Pro^{247}, Pro^{249}, Pro^{251}). Indeed, the C' secondary chemical shifts alternated in this region consistent with the fact that C^{α} atoms of residues preceding prolines show unusual chemical shifts due to the absence of an amide proton in the proline. In the case of R5 the results must be viewed with caution because of the presence of only three residues of R5 (not counting the C-terminal residue). A remarkably similar pattern is observed for K19 even though repeat R2 (exon 10) is absent (Fig. 2*C*), suggesting that the repeats represent independent structural units. A quantitative analysis of the averaged C^{α} and C' secondary chemical shifts (Fig. 2*B*) indicates that β-structure-like conformations are populated ~16, 24, and 13% of the time for residues Lys^{274}-Asp^{283}, Ser^{305}-Asp^{314}, and Gln^{336}-Asp^{345}, respectively. Besides the regions in the beginning of each repeat, residues ^{295}KDNIK^{299} and ^{357}LDNIT^{361} in repeats R2 and R4 show a stretch of negative C^{α}/C' secondary shifts, indicating a β-structure propensity. Note that no β-structure propensity is present in the corresponding region of repeat 3 (^{325}LGNIH^{329}), possibly because of the presence of a glycine (Fig. 2*B*).

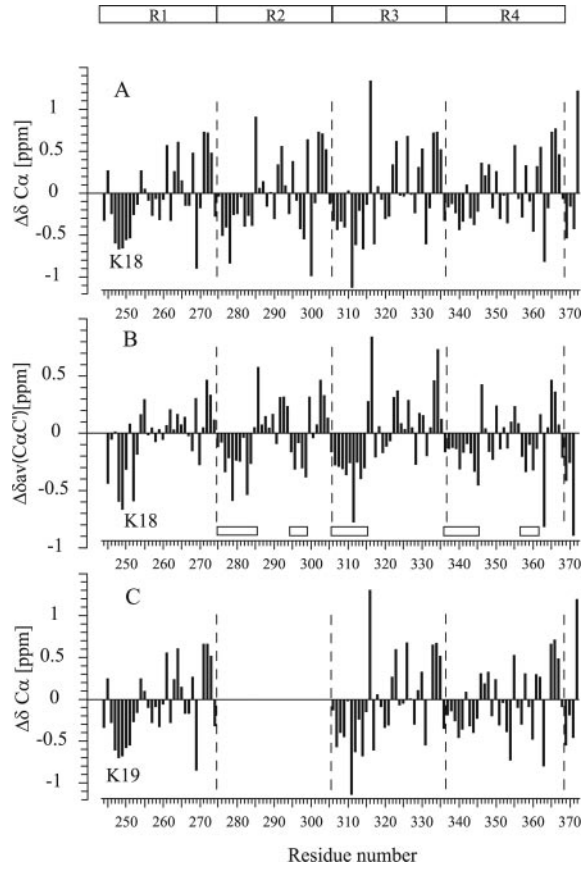

FIG. 2. **Secondary chemical shifts of tau constructs in solution.** Secondary chemical shifts for C^{α} (*A*) and averaged for C^{α} and C' (*B*) in K18 and C^{α} in K19 (*C*) recorded at 5 °C in 50 mM sodium phosphate buffer, pH 6.9, protein concentration 1 mM. The average shifts in (*B*) were calculated as $[3\Delta\delta(C^{\alpha}) + 4\Delta\delta(C')]/7$. Regions of β-structure propensity are identified by negative values of $\Delta_{av}(C^{\alpha}C')$ extending over several residues and are highlighted by *boxes* in (*B*). Repeat boundaries are indicated by *vertical dashed lines*. All glycines at position two and three in the PGGG motifs exhibited identical secondary chemical shifts.

The regions of high propensity for the β-structure are limited upstream by PGGG motifs, where the three glycines show positive C^{α} and C' secondary chemical shifts in all four repeats. This indicates either a helical propensity or a turn, in agreement with the fact that GGK and GGS sequences (present in R1 or R2) are the most common motifs in classic γ-turns. Alternatively, the PGGG motif is also common in type II β-turns. The downstream ends of the regions of high β-structure propensity are most prominently identified by positive C^{α}/C' secondary chemical shifts of the 10th and/or 11th residue in repeat 2–4 (Ser^{285}, Ser^{316}, Phe^{346}) (Fig. 2*B*). Taking further into account that sequence dyads such as ^{285}SN^{286} and ^{316}SK^{317} (the motifs following high β-propensity regions in R2 and R3) are common in type I β-turns, the C^{α} and C' secondary chemical shifts suggest a β-turn at the C-terminal end of the regions of high β-structure propensity.

In conclusion, 8–10 residues at the beginning of repeats 2–4 show a residual β-structure sandwiched between regions with a high turn propensity. The most pronounced β-structure propensity is present at the N terminus of the third repeat, whereas in the second and fourth repeat it is approximately a factor of 1.5–2 lower. These β-conformations in K18 and K19 are presumably in rapid exchange with random like structures. The C^{α} secondary chemical pattern observed for K19 is almost identical to that in K18. This indicates that the removal of the second repeat does not affect the local β-structure propensity in the remaining part of the repeat domain of tau.

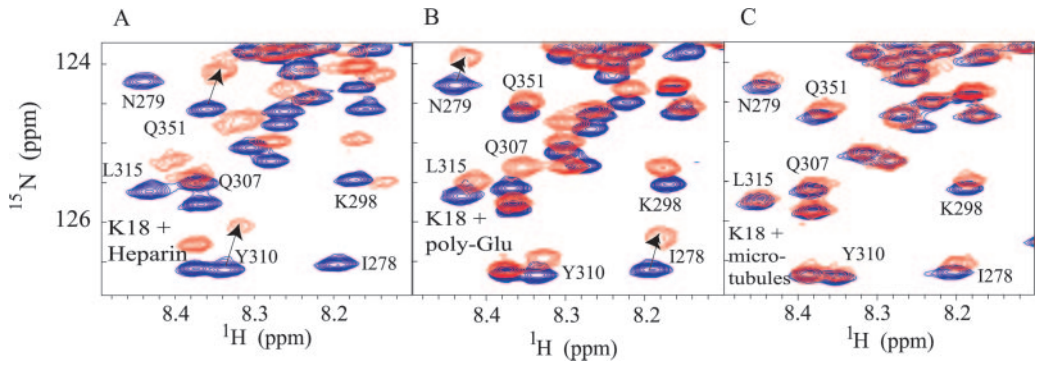

FIG. 3. **NMR titration of K18 with polyanions and MTs.** Overlay of the ^{1}H-^{15}N HSQC spectra of 0.20 mM K18 (*blue*) with 0.15 mM heparin (*red*) (*A*), 0.30 mM K18 (*blue*) with 1.3 mM poly-Glu (*red*) (*B*), and 0.13 mM K18 (*blue*) with 0.80 mM MTs (*red*) (*C*). Spectra were recorded at 5 °C in 50 mM sodium phosphate buffer, pH 6.9. Some particularly strong shifts are indicated by *arrows*. In *A* the signal of Asn^{279} (*N279*) was already attenuated below detection, indicating a chemical shift exchange intermediate on the NMR time scale.

Characterization of K18 and K19 and Its Polyanion Complexes—NMR signals of backbone amides constitute excellent probes of complex formation, providing maps of the interaction interfaces and binding constants (24). The binding of the polyanions heparin and poly-Glu to K18 and K19 was monitored by ^{1}H-^{15}N HSQC spectra. The size of the chemical shift changes for increasing polyanion concentrations depends on the binding strength to the corresponding residues. At high polyanion concentrations chemical shift changes of some residues were accompanied by a decrease of the intensity of their signals, indicating chemical shift exchange intermediate on the NMR time scale (Fig. 3).

In the case of heparin the residues exhibiting the largest displacements in the amide resonances of K18 were Val^{275}-Leu^{284} at the beginning of the second repeat (Fig. 4*A*). In addition, strong chemical shift changes were observed in the environment of selected lysine and histidine residues: Leu^{253}-Lys^{254}, His^{268}-Gln^{269}, Lys^{298}-Val^{300}, His^{329}-Lys^{331}, and His^{362}. The importance of lysine and histidine residues suggests that the binding to polyanions is electrostatically driven. Upon titration of K18 with poly-Glu, a similar pattern of chemical shift changes was observed (Fig. 4*B*), indicating that the overall binding behavior for the two types of polyanions is similar. In K19, repeat 2 is missing and can therefore not contribute to the interaction with polyanions. However, the same lysine and histidine residues as in K18 were strongly affected. In addition, slightly more pronounced chemical shift changes were observed for Val^{306}-Lys^{311}, the six residues in the third repeat that are important for tau aggregation to PHFs (Fig. 4, *C* and *D*).

Concomitant with the chemical shift changes and the disappearance of some resonances at high polyanion concentrations (caused by ligand binding), the overall signal intensity in the ^{1}H-^{15}N HSQC spectra decreased with increasing polyanion concentration (after correction for dilution effects). The latter effect is likely due to partial aggregation, because biochemical analysis indicated that at the end of the polyanion titration 50% of K18 was polymerized, as analyzed by pelleting and SDS-PAGE. A similar behavior was observed in the K19-poly-Glu titration.

To investigate the effect of aggregation further, we performed a series of ^{1}H-^{15}N HSQC spectra, in which the ratio of concentration between heparin and K18 (1:4) was held constant, and the sample was kept for variable times at 50 °C to induce and accelerate aggregation. After measurement of initial ^{1}H-^{15}N HSQCs without heparin and with a heparin:K18 ratio of 1:4 at 5 °C, the sample was heated to 50 °C and kept at this temperature for 2 h. After the 2 h the sample was cooled down to 5 °C, and an HSQC spectrum was recorded. This procedure was repeated five times, such that the protein was kept at 50 °C for 10 h in total. The addition of heparin induced the chemical shift changes that were reported in Fig. 4. The peak intensities for most residues were reduced by less than 15% upon addition of heparin with the exception of those residues showing very strong chemical shift changes. After the first 2 h at 50 °C the intensities of almost all peaks were reduced to 72% compared with the starting spectrum without heparin. There was no area in the protein that was affected particularly strongly, rather an overall loss of signal intensity was observed. At the same time, the chemical shift changes that were initially induced by addition of heparin were largely lost, *i.e.* the spectrum after 2 h at 50 °C with a heparin:K18 ratio of 1:4 was highly similar to the one of K18 before addition of heparin (shown in Fig. 3). After 4, 6, 8, and 10 h at 50 °C the overall signal intensity in ^{1}H-^{15}N HSQC spectra continuously decreased to 68, 65, 64, and 61% compared with the starting spectrum without heparin, respectively. No large chemical shift differences relative to the spectrum after 2 h at 50 °C were observed. In addition, the average transverse ^{15}N relaxation time did not change compared with free K18 upon addition of heparin or after keeping the protein up to 10 h at 50 °C (data not shown). At the end of the temperature titration biochemical analysis indicated that ~50% of K18 was polymerized. These data indicate that the observed chemical shift changes were because of the binding of the polyanion to the protein and not because of aggregation. When the protein was exposed to high levels of heparin for prolonged times or to high temperature at a constant heparin:K18 ratio of 1:4, part of the protein aggregated. As the chemical shift changes, which were induced by addition of heparin, were largely removed upon aggregation, heparin may become bound to the aggregates, thereby reducing the effective concentration of heparin in solution.

The Binding Mode of MTs and Polyanions to Tau Is Similar—The binding of K18 and K19 to MTs was characterized using the NMR chemical shift perturbation method (24) in which two-dimensional ^{1}H-^{15}N HSQC spectra of K18 and K19 were recorded in the presence of increasing amounts of taxol-stabilized MTs. The influence of temperature was probed by performing the NMR titrations at 5 and 20 °C. To ascertain the stability of the taxol-stabilized MTs at these temperatures, aliquots from the reactions of tau with MTs were characterized by sedimentation, SDS-PAGE, and electron microscopy (Fig. 5). After assembly at 37 °C the MTs exhibit the typical morphological features of protofilaments spaced ~5 nm apart. During the NMR analysis the sample is incubated for more than one h at 5 °C, but this does not lead to the disintegration of MTs in the presence of taxol (Fig. 5, *A* and *B*). In the presence of tau the surface features of MTs become somewhat fuzzier but without a change in subunit arrangement (see Santarella *et al.*, 2004

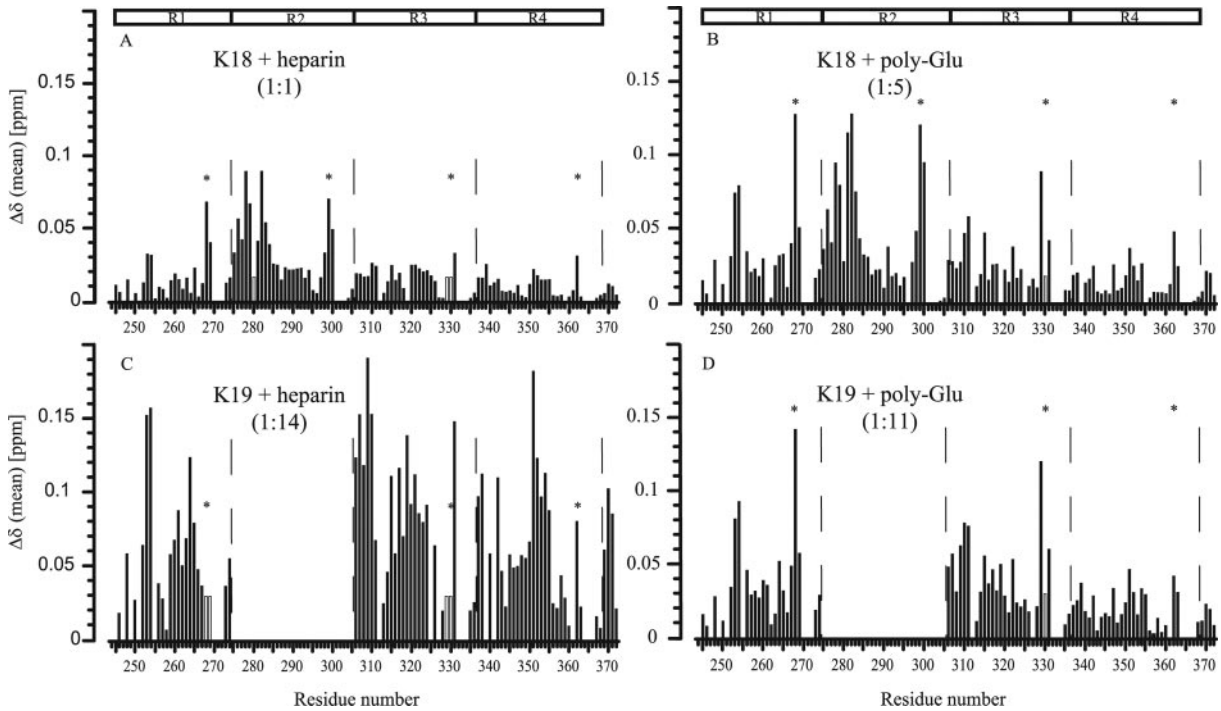

FIG. 4. **Binding of polyanions to tau.** The mean weighted ^{1}H-^{15}N chemical shifts between the ^{1}H-^{15}N HSQC spectra of free tau and tau in the presence of polyanions are shown. *A*, 0.2 mM K18 with 0.15 mM heparin (~1:1); *B*, 0.25 mM K18 with 1.3 mM poly-Glu (~1:5); *C* 0.09 mM K19 with 1.3 mM heparin (~1:14); and *D* 0.12 mM K19 with 1.35 mM poly-Glu (~1:11). Resonances that were attenuated below detection by addition of polyanions are indicated by *open bars*. Gaps are due to overlap or the presence of prolines. The average molecular weight of heparin and poly-Glu was 3000 and 10,000, respectively. Repeat boundaries are indicated by *vertical dashed lines*. * indicate histidine-lysine dyads downstream of PGGG motifs.

(39)) (Fig. 5*C*). For a quantitative analysis the samples were centrifuged, and the supernatants and pellets were checked by SDS-PAGE (Fig. 5, *D* and *E*). After MT assembly with taxol and incubation at 20 or 5 °C tubulin is found mostly in the pellet fraction (Fig. 5*D*). When increasing amounts of MTs were added to K18, the binding resulted in increasing amounts of K18 in the pellet fraction (Fig. 5*D*). The same was true for K19. These experiments show that the taxol-stabilized MTs persist over the time course of the NMR measurement and that binding parameters of both K19 and K18 are in good agreement with earlier results (3).

Continuous chemical shift changes of selected residues followed by the disappearance of the most strongly shifting resonances, especially at 20 °C, were observed. In addition, the signal:noise ratio rapidly decreased at high MT concentrations, indicative of an increasing amount of K18 or K19 bound to MTs. When bound to MTs, the NMR signals of K18 or K19 are not observable because of very fast relaxation.

At 5 °C the most strongly shifting resonances in K18 were found mainly in the environment of lysine and histidine residues: Leu^{253}-Lys^{254}, His^{268}-Gln^{269}, Lys^{298}-Val^{300}, His^{329}-Lys^{331}, and His^{362} (Fig. 6*A*). This indicates that each repeat contains a binding site for anchoring K18 to MTs. In agreement with the repetitive nature of the repeat region, these anchors are primarily located at equivalent positions in each repeat, just N-terminal to the PGGG motif. The same lysine and histidines resonances were affected at 20 °C, although to a lesser extent. At 20 °C the most pronounced chemical shift changes were observed for residues Lys^{274}-Leu^{284} at the beginning of the second repeat (Fig. 6*B*). Within this region Ile^{278} and Asn^{279}, together with Lys^{281} and Leu^{282} displayed the strongest chemical shift changes, whereas Lys^{280} was only weakly affected by the addition of MTs.

In the K18-MT titration, only minor chemical shift changes were observed for resonances located in the beginning of repeat 3. Addition of heparin to K19, on the other hand, had a pronounced effect on residues Val^{306}-Lys^{311}. In addition, slightly stronger chemical shift changes were observed for these residues in the K19-MT titration (Fig. 6*B* and supplemental Fig. S2). Further evidence for the involvement of the N-terminal part of the third repeat into binding to MTs comes from the decrease of the signal intensity for increasing MT concentrations. The signal intensity for residues Val^{306}-Lys^{311} decreased as quickly as that of the interacting part of the second repeat, *i.e.* the site that showed the strongest chemical shift changes upon addition of MTs to K18, and decreased more rapidly than the intensity for other residues in the K19-MT titration (supplemental Fig. S3). Overall, the pattern of chemical shift changes induced by addition of MTs was very similar for K18 and K19 (Fig. 6, *A* and *C*).

We concluded that repeats R1–R4 of four-repeat tau are attached to MTs mainly via the positive charges just upstream of the PGGG motif. The attachment of repeat one is further stabilized by electrostatic interactions involving the positive charge of Lys^{254}. In addition, the region Lys^{274}-Leu^{284} is important for binding to MTs. An additional MT-binding site is located in the beginning of the third repeat, which it is particularly important for binding of three-repat tau to MTs.

DISCUSSION

Tau is an interesting protein from several different perspectives. First, tau is one of the major microtubule-associated proteins in the brain; it plays a prominent role in the formation of axons and is therefore important for understanding neuronal cell biology and brain development. Secondly, tau is a prototype of the emerging class of "natively unfolded" or "intrinsically unstructured" proteins whose properties are not accessible by x-ray crystallography. Thirdly, from a medical perspective tau represents one of the hallmarks of Alzheimer disease, the most common form of dementia, where it forms pathological protein

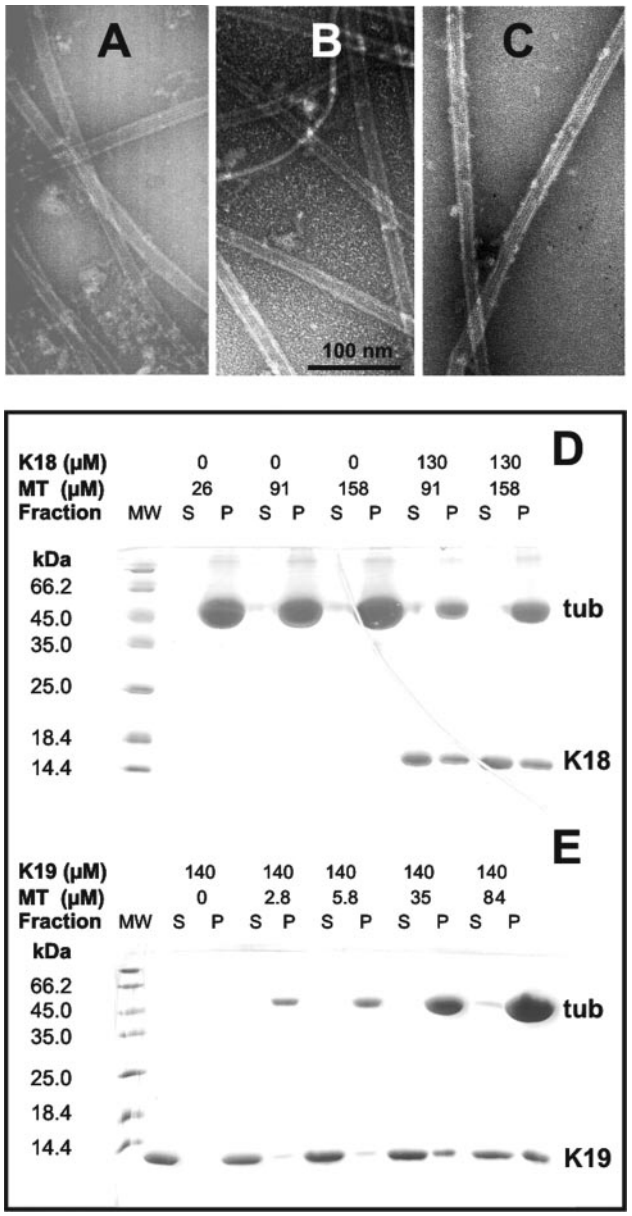

FIG. 5. **Analysis of MT stability and interaction with tau by electron microscopy and SDS-PAGE.** *A*, the morphology of MTs after assembly at 37 °C exhibit the typical features of MTs with a width of about 25–28 nm and 6–7 visible protofilaments. After incubation at 4 °C the morphology is not altered (*B*). In the presence of tau (*C*) the surface of the MTs appears fuzzier than in the absence of tau. *Bar* = 100 nm. The stability of MTs at different concentrations and the interaction with K18 (130 μM) was further analyzed by centrifugation (100,000 × *g* for 1 h at 4 °C) and subsequent SDS-PAGE on 17% SDS gels. *D*, MTs pelleted after incubation at 20 and 5 °C (*lanes 2–7*). Samples of the interaction studies were directly centrifuged after the NMR analysis (*lanes 8–11*). *E*, similar analysis of the interaction between K19 and MT s. K19 at a fixed concentration (140 μM) was incubated with increasing concentrations of MTs and after centrifugation supernatants, and pellets were applied to a 17% SDS-PAGE. *tub*, tubulin.

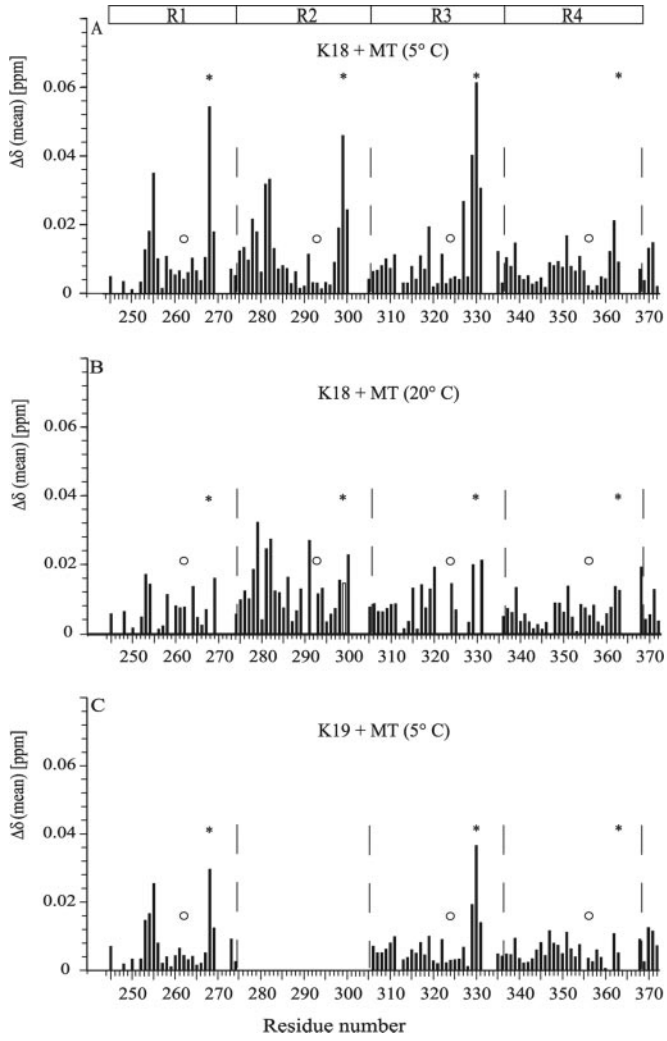

FIG. 6. **Binding of tau to preassembled MTs.** Mean weighted ^{1}H-^{15}N chemical shifts between the ^{1}H-^{15}N HSQC spectra of free tau and tau in the presence of MTs. *A*, 0.13 mM K18 with 79 μM MTs at 5 °C; *B*, 0.13 mM K18 with 79 μM MTs at 20 °C; and *C*, 0.14 mM K19 with 35 μM MTs at 5 °C. Resonances that were attenuated beyond detection by addition of MTs are indicated by *open bars*. Gaps are due to overlap or the presence of prolines. Repeat boundaries are marked by *vertical dashed lines*. * and ° indicate histidine-lysine dyads downstream of PGGG motifs and serines known to be phosphorylated, respectively.

aggregates that are toxic to the neurons. These reasons prompted us to apply state of the art, multidimensional NMR spectroscopy, with the aim of identifying the structural features of tau that are responsible for its physiological and pathological roles. In the present study we focus on the repeat domain of tau that forms the core of the MT-binding domain as well as the core of Alzheimer paired helical filaments (PHFs). We have used NMR spectroscopy to detect structural motifs and potential seeds of aggregation in the repeat region of tau and to characterize its interaction with MTs and certain polyanions that are known to promote the aggregation into PHFs.

The major results can be summarized as follows (Fig. 7). 1) The beginning of each repeat is characterized by a stretch of 8–10 residues with negative secondary chemical shift values. For the case of R2–R4 this indicates a high propensity of β-structure. These regions coincide with sequence motifs known to be involved in the abnormal aggregation of tau. The β-forming motifs are sandwiched between motifs that have a high propensity for turns and therefore interrupt the β-conformation (*e.g.* the PGGG motifs). Additional stretches of β-propensity occur upstream of the PGGG motifs in repeats R2 and R4. 2) The conformational preferences are the same in different variants of tau with 3 or 4 repeats (corresponding to fetal or adult tau). This suggests that the repeats behave like independent-folding units. 3) MTs and other polyanionic binding partners of tau show similar preferred regions of interaction. They include the beginning of repeats R2 and R3 (coincident with the PHF-forming hexapeptide motifs) and spots of high positive charge upstream of the PGGG motifs. This supports the view that the abnormal aggregation (caused by polyanionic cofac-

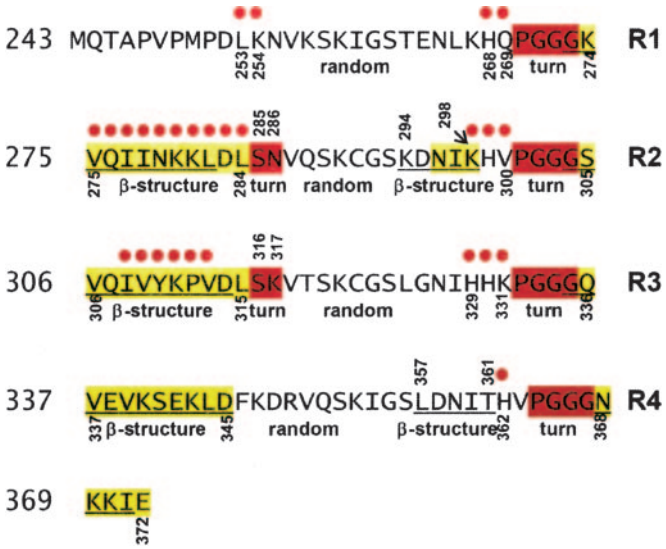

FIG. 7. **Summary of results.** The sequence of the four repeats of K18 plus the adjacent four amino acids is shown ordered by the repeat structure. The residues of special significance are *highlighted*. *Red* amino acids are likely to be involved in turn structures, *e.g.* the PGGG motifs at the end of each repeat. *Yellow* amino acids show a negative secondary C^{α} shift, *underlined* residues exhibit a negative secondary C′ chemical shift. At the beginning of R2, R3, and R4 there are regions of 8–10 residues with negative secondary C^{α} chemical shifts and negative secondary C′ chemical shifts, indicating a residual β-structure. The middle of R2 and R4 contain a further short stretch with negative secondary C′-shifts. The binding sites for polyanions (heparin, poly-Glu, and MTs) are marked by *red circles* above the sequence.

tors) is based on the same structural features as the physiological interaction with MTs.

Soluble Tau Contains Residual β-Structure Providing Seeds of Aggregation—To allow a high-resolution characterization by NMR, it was necessary to assign the backbone resonances of all residues. Previously, the NMR resonances of single residues, at most dipeptides, were assigned unambiguously covering only 12% of the repeat domain of tau. These isolated assignments did not provide any indication for residual structure (25). Despite the high degree of overlap caused by the absence of a well defined secondary and three-dimensional structure, we were able to fully assign the backbone resonances of K18 and K19. NMR chemical shifts are sensitive probes for the environments of nuclei. Comparison of the assigned backbone resonances showed that signals of Val^{275} and Gln^{276} at the beginning of R2 in K18 were exactly coincident with the signals of Val^{306} and Gln^{307} at the beginning of R3 in K19. Either the chemical shifts are dominated by the local sequence composition or any potentially present residual structure is very similar in K18 and K19.

At the beginning of repeats R2, R3, and R4 a significant propensity for β-structure within continuous stretches of 8–10 residues could be identified (16, 24, and 13%, respectively). These β-regions terminate on both ends by motifs with a high propensity for turns, such as the PGGG motifs or the SN or SK dyads. The β-structure propensity is most pronounced (~24%) for residues Ser^{305}-Asp^{314} in the beginning of R3. Note that this is an average value calculated for all residues within this regions, and it does not necessarily indicate that all residues populate β-structure at the same time. In addition, negative secondary chemical shifts for residues ^{295}KDNIK^{299} and ^{357}LDNIT^{361} suggest a weak propensity for β-structure in the C-terminal half of repeats R2 and R4. These findings are in agreement with other data (x-ray scattering, CD, gel filtration, secondary structure predictions, etc.) indicating that tau has a very low content of secondary structure (Schweers *et al.* (7)).

While this manuscript was in preparation an NMR study of K19 was published (26). Similar to our results, these authors observed a tendency to form β-structure in the beginning of R3. No tendency to form a β-structure is reported for R4. In addition, as only K19 was studied, neither the structural properties of R2 nor any isoform-specific differences between three- and four-repeat tau could be addressed. Most strikingly, however, Eliezer *et al.* (26) concluded that much of K19, comprising residues 253–267, 315–328, and 346–361, preferentially populates helical conformations. This conclusion was based mainly on long stretches of positive C^{α} secondary chemical shifts. We were not able to observe such positive C^{α} secondary chemical shifts (Fig. 2*A*), despite the fact that our pattern of C′ secondary chemical shifts is very similar to that reported by Eliezer *et al.* (26) (supplemental Fig. S1). Our data are in agreement with earlier results obtained by CD and FTIR spectroscopy, in which no helical propensities were detected for monomeric K18 or K19 (13). In addition, we have characterized the interaction of K18 and K19 with polyanions and microtubules, and the high degree of similarity between the binding of polyanions and microtubules suggests that stable microtubules prevent PHF formation by blocking the tau-polyanion interaction sites, which are crucial for PHF formation (see below).

The partially populated β-structure at the beginning of R2 and R3 is also consistent with the essential role of two hexapeptide motifs, ^{275}VQIINK^{280} and ^{306}VQIVYK^{311}, for the assembly of tau into PHFs. ^{306}VQIVYK^{311} represents the minimal hexapeptide motif for tau-tau interaction and is capable of inducing tau aggregation. In addition, a 43-residue fragment of K19, which contains the third repeat of tau and some flanking residues, acquires a pronounced β-structure in conditions of self-assembly (8). The key role of the hexapeptide ^{306}VQIVYK^{311} in R3 for PHF aggregation and its pronounced β-structure propensity is also in agreement with data on peptide fragments comprising a single repeat: Trifluoroethanol at low concentrations only induced an α-helical structure in the hexapeptide in R2 but not in ^{306}VQIVYK^{311} in R3 (27, 28). Furthermore, the isolated hexapeptides ^{275}VQIINK^{280} and ^{306}VQIVYK^{311} are able to polymerize with formation of β-structure (13, 14).

Several mutations in the tau gene have been linked to frontotemporal dementias and parkinsonism (FTDP-17 (29)). Their mode of action may not be uniform, but some of them appear to enhance aggregation by increasing the β-structure propensity within the repeat domain. This holds particularly for the mutations ΔK280 and P301L, which are located in or near the regions with high β-structure propensity in the wild-type protein (13). A higher β-structure propensity leads to more molecules that preferentially adopt a β-structure thereby increasing the rate of aggregation. Conversely, proline mutants introduced into these regions disrupt the β-propensity and thus render the molecule largely incapable of PHF formation (8). The repeat region of four-repeat tau contains two cysteines whose cross-linking strongly attenuates aggregation by formation of an inactive monomer (6). These two cysteines are just C-terminal of the regions of high β-propensity. This suggest that cross-linking of these cysteines brings together the regions of high β-propensity in repeats R2 and R3 forming a partially populated intramolecular β-sheet. Such an intramolecular β-sheet would reduce the tendency to form PHFs, as PHF assembly requires the formation of intermolecular H-bonds within these regions. On the other hand, cross-linking of tau molecules into dimers by intermolecular disulfide bonds can bring regions of high β-propensity close together. This would favor formation of intermolecular β-sheets in agreement with a strong enhancement of aggregation by dimerization (12).

Regions with β-Structure Propensity Coincide with Binding Sites to Polyanions—PHFs isolated from the brains of patients with Alzheimer disease are not only composed of tau molecules but contain other nonprotein components, including heparan, a glycosaminoglycan, the more extensively sulfated form of which is heparin. *In vitro*, heparin and other polyanions, such as poly-Glu and RNA, greatly improve polymerizability of tau. This is thought to be because of a neutralization of positive residues as the enhancement is not restricted to a specific polyanion (30–32). Our results show that the binding of polyanions is concentrated around positively charged patches, including the KK motif (280–281) at the beginning of repeat R2, and the KH (267–268, 298–299) or HHK (329–331) motifs near the end of R1, R2, and R3. By comparison, single positive charges in equivalent locations have a much weaker effect on binding (*e.g.* Lys^{311} at the beginning of R3, or His^{362} near the end of R4). The patterns of the altered backbone chemical shifts mapped onto the primary sequence (Fig. 4, *A* and *B*) were very similar for heparin and poly-Glu, suggesting a common mode of binding dictated largely by electrostatic interactions.

The binding of polyanions to the positively charged amino acids reduces the net charge and therefore decreases the propensity for random coil (33). Additionally the binding to the sites of residual β-structure might help to stabilize the β-conformation and might thereby allow interaction of the β-strand with other tau molecules. Thus, polyanions enhance aggregation by directly stabilizing the regions which are essential for aggregation. This is opposite to the interaction of α-synuclein with polyamines, which bind to the C-terminal domain of α-synuclein, cause a release of an autoinhibitory residual structure, and render the hydrophobic patches of the NAC (Non-Aβ component of Alzheimer disease amyloid) region accessible, such that α-synuclein is able to adopt β-sheet conformations conductive of aggregation (34).

MTs Prevent PHF Formation by Blocking the Tau-Polyanion Interaction Sites That Are Crucial for PHF Formation—Tau is a microtubule-associated protein that regulates diverse and essential MT functions, including polymerization and stabilization of MT and modulation of MT dynamics. Mutations in tau associated with frontotemporal dementia with parkinsonism linked to chromosome 17 (FDTP-17) weaken the interaction between tau and MTs and cause a decrease in MT stabilization (35). Therefore, knowledge of the detailed mechanism by which tau binds to MTs is highly important. In the study presented herein we have characterized the reversible binding of tau to preassembled, taxol-stabilized MTs on the level of individual tau residues. Because it has been demonstrated previously that the repeat domain of tau is important for MT binding activity, we targeted our high-resolution study to this region of the protein.

The NMR titrations identified residues Lys^{274}-Leu^{284} as an important region of tau for binding to MTs. This is in agreement with truncation analyses by Goode *et al*. (36, 37). A 2.3- and 3.1-fold reduction of MT binding affinity, which was observed when mutating Lys^{274} or Lys^{281} to alanine, correlates well with the strong chemical shift changes observed for Ile^{278} and Lys^{281} upon addition of MTs. In addition, Lys^{280} showed only small chemical shift changes, consistent with a smaller contribution to binding affinity as indicated by site-directed mutagenesis. Besides these strong electrostatic interactions involving the N-terminal part of R2, the NMR data show that the tau-MT interaction is further enhanced by discrete interaction clusters of positive charges upstream of the PGGG motifs.

To investigate isoform-specific differences in MT binding affinity, we also studied the interaction of K19 with MTs. Previously, it was shown that the C-terminal sequences downstream of the repeat region make a strong but indirect contribution to MT binding affinity in three-repeat tau, whereas in four-repeat tau they almost have no effect. The K19 construct does not include these C-terminal sequences. However, the K19-MT NMR data give insight on a residue basis and can be used to probe for local changes in the MT interaction. The highly similar pattern of chemical shift changes in K18 and K19 upon addition of MTs suggests that the lysine-histidine binding sites upstream of the PGGG motifs, contribute independently to the interaction.

Our study does not directly address the nature of the tau binding sites on tubulin and MTs. It is commonly accepted that tau interacts with the C terminus of tubulin that is believed to be exposed on the surface of MTs (38). Comparison of chemical shift changes observed for K18 and K19 upon addition of MTs with those observed upon addition of polyanions indicate a very similar binding mode. Considering that poly-Glu resembles the Glu-rich C-terminal sequence of tubulin, the NMR data suggest that the positively charged clusters described above bind to the C terminus of tubulin. The similar binding mode of tau to MTs and polyanions also supports the hypothesis that stable MTs prevent PHF formation by blocking the tau-polyanion interaction sites, which are crucial for PHF formation.

It is known that phosphorylation at K*X*GS motifs regulate affinity of tau to MTs (4). We have shown that the repeat domain of tau binds to MTs through spots of high positive charge comprising the beginning of R2 and R3, as well as histidine-lysine regions upstream of the PGGG motifs. Serine 262, 293, 324, and 356 are separated by only four residues from these histidine-lysine regions carrying two to three positive charges at the C-terminal end of each repeat. Thus the effect of phosphorylation can be achieved, because the introduction of the negative charge of the phosphate group partially neutralizes the positive spots required for MT binding. This intramolecular charge neutralization might be favored by the high flexibility of the protein backbone of tau, which allows the spots of positive and negative charges to come close together. Even more, the high flexibility of tau might actually be required to allow a detailed control of the tau-MT interaction by phosphorylation. In addition, the attraction between the phosphate and the positively charged lysine-histidine region might force a turn, reducing the propensity for β-structure, which was observed for residues ^{295}KDNIK^{298} and ^{357}LDNIT^{361} and might alter the distances between the distributed weak interaction sites in a way that they no longer fit to their interaction sites on the MT surface.

The investigations featured above provide a detailed novel view of the native state of the repeat region of the microtubule-associated protein tau and its interaction with polyanions and MTs. The presence of seeds of aggregation at the beginning of repeats R2 and R3 (hexapeptide motifs), which coincide with the observed propensity for β-structure and the binding regions of tau to MTs and polyanions, stresses the importance of these regions for their normal MT regulating function and for their involvement in the neurodegenerative process in which tau is assembled into Alzheimer paired helical filaments. The results presented in this study will be important when assessing factors or drugs designed to suppress the aggregation of tau in neurons, and thus to prevent one of the crucial steps in Alzheimer's disease.

Acknowledgments—We thank Sabrina Hübschmann, Bianca Wichmann, Vinesh Vijayan, and Dirk Lennartz for excellent technical assistance, Stefan Schwarzinger for help with the analysis of chemical shift values, and Eva-Maria Mandelkow for advice throughout the project. The work was done within the scientific scope of the DFG Center for Molecular Physiology of the Brain (CMPB) in Göttingen.

REFERENCES

1. Selkoe, D. J., and Schenk, D. (2003) *Annu. Rev. Pharmacol. Toxicol.* **43,** 545–584
2. Mandelkow, E. M., and Mandelkow, E. (1998) *Trends Cell Biol.* **8,** 425–427
3. Gustke, N., Trinczek, B., Biernat, J., Mandelkow, E. M., and Mandelkow, E. (1994) *Biochemistry* **33,** 9511–9522
4. Biernat, J., Gustke, N., Drewes, G., Mandelkow, E. M., and Mandelkow, E. (1993) *Neuron* **11,** 153–163
5. Schneider, A., Biernat, J., von Bergen, M., Mandelkow, E., and Mandelkow, E. M. (1999) *Biochemistry* **38,** 3549–3558
6. Barghorn, S., and Mandelkow, E. (2002) *Biochemistry* **41,** 14885–14896
7. Schweers, O., Schonbrunn-Hanebeck, E., Marx, A., and Mandelkow, E. (1994) *J. Biol. Chem.* **269,** 24290–24297
8. von Bergen, M., Friedhoff, P., Biernat, J., Heberle, J., Mandelkow, E. M., and Mandelkow, E. (2000) *Mol. Biol. Cell* **11,** 363A-363A
9. Buee, L., Hamdane, M., Delobel, P., Sambo, A. V., Begard, S., Ghestem, A., Sergeant, N., and Delacourte, A. (2002) *J. Soc. Biol.* **196,** 103–108
10. Wischik, C. M., Novak, M., Thogersen, H. C., Edwards, P. C., Runswick, M. J., Jakes, R., Walker, J. E., Milstein, C., Roth, M., and Klug, A. (1988) *Proc. Natl. Acad. Sci. U. S. A.* **85,** 4506–4510
11. Wille, H., Drewes, G., Biernat, J., Mandelkow, E. M., and Mandelkow, E. (1992) *J. Cell Biol.* **118,** 573–584
12. Friedhoff, P., von Bergen, M., Mandelkow, E. M., Davies, P., and Mandelkow, E. (1998) *Proc. Natl. Acad. Sci. U. S. A.* **95,** 15712–15717
13. von Bergen, M., Barghorn, S., Li, L., Marx, A., Biernat, J., Mandelkow, E. M., and Mandelkow, E. (2001) *J. Biol. Chem.* **276,** 48165–48174
14. Goux, W. J., Kopplin, L., Nguyen, A. D., Leak, K., Rutkofsky, M., Shanmuganandam, V. D., Sharma, D., Inouye, H., and Kirschner, D. A. (2004) *J. Biol. Chem.* **279,** 26868–26875
15. Mandelkow, E. M., Herrmann, M., and Ruhl, U. (1985) *J. Mol. Biol.* **185,** 311–327
16. Delaglio, F., Grzesiek, S., Vuister, G. W., Zhu, G., Pfeifer, J., and Bax, A. (1995) *J. Biomol. NMR* **6,** 277–293
17. Schwarzinger, S., Kroon, G. J. A., Foss, T. R., Chung, J., Wright, P. E., and Dyson, H. J. (2001) *J. Am. Chem. Soc.* **123,** 2970–2978
18. Wishart, D. S., and Sykes, B. D. (1994) *Methods Enzymol.* **239,** 363–392
19. Bax, A., and Grzesiek, S. (1993) *Acc. Chem. Res.* **26,** 131–138
20. Zweckstetter, M., and Bax, A. (2001) *J. Am. Chem. Soc.* **123,** 9490–9491
21. Panchal, S. C., Bhavesh, N. S., and Hosur, R. V. (2001) *J. Biomol. NMR* **20,** 135–147
22. Jung, Y. S., and Zweckstetter, M. (2004) *J. Biomol. NMR* **30,** 11–23
23. Dyson, H. J., and Wright, P. E. (1998) *Nat. Struct. Biol.* **5,** (suppl.) 499–503
24. Craik, D. J., and Wilce, J. A. (1997) *Methods Mol. Biol.* **60,** 195–232
25. Smet, C., Leroy, A., Sillen, A., Wieruszeski, J. M., Landrieu, I., and Lippens, G. (2004) *Chembiochem* **5,** 1639–1646
26. Eliezer, D., Barre, P., Kobaslija, M., Chan, D., Li, X., and Heend, L. (2005) *Biochemistry* **44,** 1026–1036
27. Hiraoka, S., Yao, T. M., Minoura, K., Tomoo, K., Sumida, M., Taniguchi, T., and Ishida, T. (2004) *Biochem. Biophys. Res. Commun.* **315,** 659–663
28. Minoura, K., Yao, T. M., Tomoo, K., Sumida, M., Sasaki, M., Taniguchi, T., and Ishida, T. (2004) *Eur. J. Biochem.* **271,** 545–552
29. Higuchi, M., Lee, V. M., and Trojanowski, J. Q. (2002) *Neuromolecular Med.* **2,** 131–150
30. Goedert, M., Jakes, R., Spillantini, M. G., Hasegawa, M., Smith, M. J., and Crowther, R. A. (1996) *Nature* **383,** 550–553
31. Kampers, T., Friedhoff, P., Biernat, J., Mandelkow, E. M., and Mandelkow, E. (1996) *FEBS Lett.* **399,** 344–349
32. Perez, M., Valpuesta, J. M., Medina, M., Montejo de Garcini, E., and Avila, J. (1996) *J. Neurochem.* **67,** 1183–1190
33. Uversky, V. N., Gillespie, J. R., and Fink, A. L. (2000) *Proteins* **41,** 415–427
34. Bertoncini, C. W., Jung, Y. S., Fernandez, C. O., Hoyer, W., Griesinger, C., Jovin, T. M., and Zweckstetter, M. (2005) *Proc. Natl. Acad. Sci. U. S. A.* **102,** 1430–1435
35. Hasegawa, M., Smith, M. J., and Goedert, M. (1998) *FEBS Lett.* **437,** 207–210
36. Goode, B. L., Chau, M., Denis, P. E., and Feinstein, S. C. (2000) *J. Biol. Chem.* **275,** 38182–38189
37. Goode, B. L., and Feinstein, S. C. (1994) *J. Cell Biol.* **124,** 769–782
38. Downing, K. H., and Nogales, E. (1999) *Cell Struct. Funct.* **24,** 269–275
39. Santarella, R. A., Skiniotis, G., Goldie, K. N., Tittmann, P., Gross, H., Mandelkow, E. M., Mandelkow, E., and Hoenger, A. (2004) *J. Mol. Biol.* **339,** 539–553